ELSEVIER



# Graphene: a new emerging lubricant☆

**Diana Berman[1], Ali Erdemir[2] and Anirudha V. Sumant[1,*]**

[1] Center for Nanoscale Materials, Argonne National Laboratory, 9700 South Cass Avenue, Argonne, IL 60439, United States
[2] Energy Systems Division, Argonne National Laboratory, 9700 South Cass Avenue, Argonne, IL 60439, United States

**In recent years, reducing friction and wear-related mechanical failures in moving mechanical systems has gained increased attention due to friction's adverse impacts on efficiency, durability, and environmental compatibility. Accordingly, the search continues for novel materials, coatings, and lubricants (both liquid and solid) that can potentially reduce friction and wear. Despite intense R&D efforts on graphene for a myriad of existing and future applications, its tribological potential as a lubricant remains relatively unexplored. In this review, we provide an up-to-date survey of recent tribological studies based on graphene from the nano-scale to macro-scale, in particular, its use as a self-lubricating solid or as an additive for lubricating oils.**

## Introduction

Increasing transportation and other industrial activities since the beginning of the last century have been consuming much of our non-renewable energy resources (like petroleum) day by day, and a significant portion of the energy produced is spent overcoming friction in moving mechanical systems. More important, much of the fuel used to generate energy turns into $CO_2$, which contributes to climate change and could have dire consequences [1]. Accordingly, more effective control or reduction of friction in moving mechanical systems is very important for a sustainable future.

Frequently encountered in our daily activities, friction is a fact of life. Sliding, rolling, or rotating contact interfaces in every man-made, natural or biological system generate friction. If not reduced or controlled effectively, high friction often leads to higher wear losses and, hence, shorter life and poor reliability. Consequently, friction has been one of the most active fields of study in the past. Many researchers are still working to understand the root causes of friction and new ways to nearly eliminate it to achieve much higher efficiency and longer durability in all types of moving mechanical systems [2].

One of the most effective ways to control friction is to use a lubricant in liquid and/or solid forms. Even certain gases may be used to lubricate rubbing surfaces. Liquid lubricants reduce friction by preventing sliding contact interfaces from severe or more frequent metal-to-metal contacts or by forming a low-shear, high-durability boundary film on rubbing surfaces. For example, depending on the sliding speed and other operating conditions, engine oils can effectively separate the contacting surfaces of rings and liners and, thereby, reduce the frequency of direct metal-to-metal contact and thus friction and wear. If and when there is metal-to-metal contact, the additives in these oils form a low-shear, highly protective boundary film to provide additional safety. In short, reducing friction means higher fuel savings; reducing wear means longer durability. Thanks to these solid and liquid lubricants, machine components of today's engines and other mechanical systems operate safely and smoothly for a long time.

Liquid lubricants are delivered to sliding interfaces through a pump or by other kinds of oil delivery mechanisms, while solid lubricants have to be applied as thin films using physical vapor deposition (PVD) and/or chemical vapor deposition (CVD) methods. Due to their finite thickness, solid lubricant films wear out eventually and lose their effectiveness. They are also very sensitive



*Corresponding author:. Sumant, A.V. (sumant@anl.gov)

to the test environments; in fact, some of them, like $MoS_2$, will not lubricate or last long if oxygen and/or water molecules are present; indeed, graphite and boric acid will not function without humidity in the surrounding air [3]. Therefore, the most desirable solid lubricant is environmentally insensitive, highly durable, and easy to deliver to the contact interfaces. In this review, we will make a case that graphene can provide extreme resistance to wear (as much as four orders of magnitude reduction in wear) regardless of test environments while not posing adverse environmental effects. Graphene, a two-dimensional carbon material, was stably isolated only in 2004 [4] but has already attracted significant attention in many different fields. Of these, tribological applications are still the least explored. With this review, we intend to highlight graphene's unusual properties to reduce wear and friction in nano-scale to macro-scale systems. Overall, we will show that graphene has much to offer as a high-performance solid lubricant or as an additive in liquid lubricants.

## Why graphene?

Graphene being two-dimensional material, offers unique friction and wear properties that is not typically seen in conventional materials. Besides its well-established thermal, electrical, optical, and mechanical properties, graphene can serve as a solid or colloidal liquid lubricant. Its high chemical inertness, extreme strength, and easy shear capability on its densely packed and atomically smooth surface are the major favorable attributes for its impressive tribological behavior. Since it is ultrathin even with multilayers, it can be applied to nano-scale or micro-scale systems such as microelectromechanical systems (MEMS) and nanoelectromechnical systems (NEMS) with oscillating, rotating, and sliding contacts to reduce stiction, friction, and wear.

First of all, the extreme mechanical strength of graphene suppresses material wear. For example, Lee et al. [5] tested the mechanical properties of graphene and confirmed it to be one of the strongest materials ever measured. For their study, the authors used free-standing graphene membranes and analyzed them with a diamond atomic force microscopy (AFM) probe, which allowed measuring the breaking strength. The measured strength of defect-free graphene sheet corresponds to a Young's modulus of 1 TPa. The breaking force depends on the tip radius, not the diameter of the membrane. Moreover, it was shown recently that the grain boundaries do not affect the overall strength of graphene [6], even though the introduction of other kinds of defects (such as oxidation) largely contributes to the mechanical properties of graphene and decreases its strength and stiffness. From a tribological point of view, such extreme mechanical strength is highly desirable for wear protection.

Secondly, graphene has been shown to be impermeable to liquids and gases [7], such as water or oxygen, thus slowing down the corrosive and oxidative processes that usually cause more damage to rubbing surfaces. Moreover, liquid water has been shown to minimize friction on graphene [8], thus presumably limiting the effect of capillary forces typical of humid environments. Singh et al. [8] demonstrated that the wetting angle is affected by the surface underneath the graphene layer; however, the effect of the substrate is modified by the number of layers and is negligible for multiple layers of graphene. Also, graphene is an atomically smooth two-dimensional material with low surface energy and is, therefore, able to replace the thin solid films usually used for reducing adhesion and friction of various surfaces.

All the properties mentioned above make graphene very attractive for demanding tribological applications to achieve low friction and low wear regimes.

## Graphene synthesis

Different production methods are available for graphene. Depending on the type and the quality, the properties of the synthesized graphene may vary a great deal; in particular, the grain size, shape, thickness, and the density of defects change and thus affect the graphene's mechanical and tribological properties.

Initially, graphene was produced by the so-called 'scotch-tape' or mechanical exfoliation method [9], where commercially available adhesive tape is used to peel multiple layers from a highly ordered pyrolytic graphite (HOPG) and to transfer them by pressing the tape onto the desired substrate. Since then the number of methods for graphene production has significantly increased. Some of these include dry mechanical [4,10] or chemical [11,12] exfoliation; unrolling/unzipping of carbon nanotubes (CNTs) through a variety of ways such as electrochemical, chemical or physical methods [13]; CVD [14,15] or epitaxial growth [16]; arc discharge; the reduction of graphene oxide [17,18]; and many other organic synthetic methods. Widely used CVD methods are able to synthesize high-quality graphene on the catalytic surface, such as nickel or copper, in the presence of a carbon supply such as hydrocarbon gases [19]. In Fig. 1, Raman spectroscopy is used for analyzing the defects in the synthesized graphene, as well as the number of deposited graphene layers [20].

## Graphene as a solid lubricant: from nano-scale to macro-scale

Unique physical, mechanical, and chemical properties of graphene make it an attractive candidate for many tribological applications where control of friction and wear is of paramount importance at different length scales. In the following sub-sections, we review the tribological performance of graphene from nano-scale to micro-scale and up to macro-scale.

### *Graphene tribology at nano-scale and micro-scale*

The atomically thin nature of graphene and its ability to conformally coat micro-scale and nano-scale objects simply by dispensing graphene flakes via solution make it a potential low friction and wear resistance coating that would extend the lifetime of MEMS/NEMS devices and constitute the motivation behind current studies being carried out in this direction.

### Nano-scale studies

Often, theoretical predictions drive future experiments and usage of novel materials. In the case of graphene, several studies predicted the nature of the graphene's friction mechanism based upon a variety of computational methods at scales varying from sub-nano up to meso [21–26].

In most of the nano-scale computational and experimental studies on graphene, the tribological behavior was shown to depend on stacking and other structural features, as well as the nature of the sliding surfaces. This observation is clearly seen for two different systems: (a) the friction of a nano-scale AFM tip

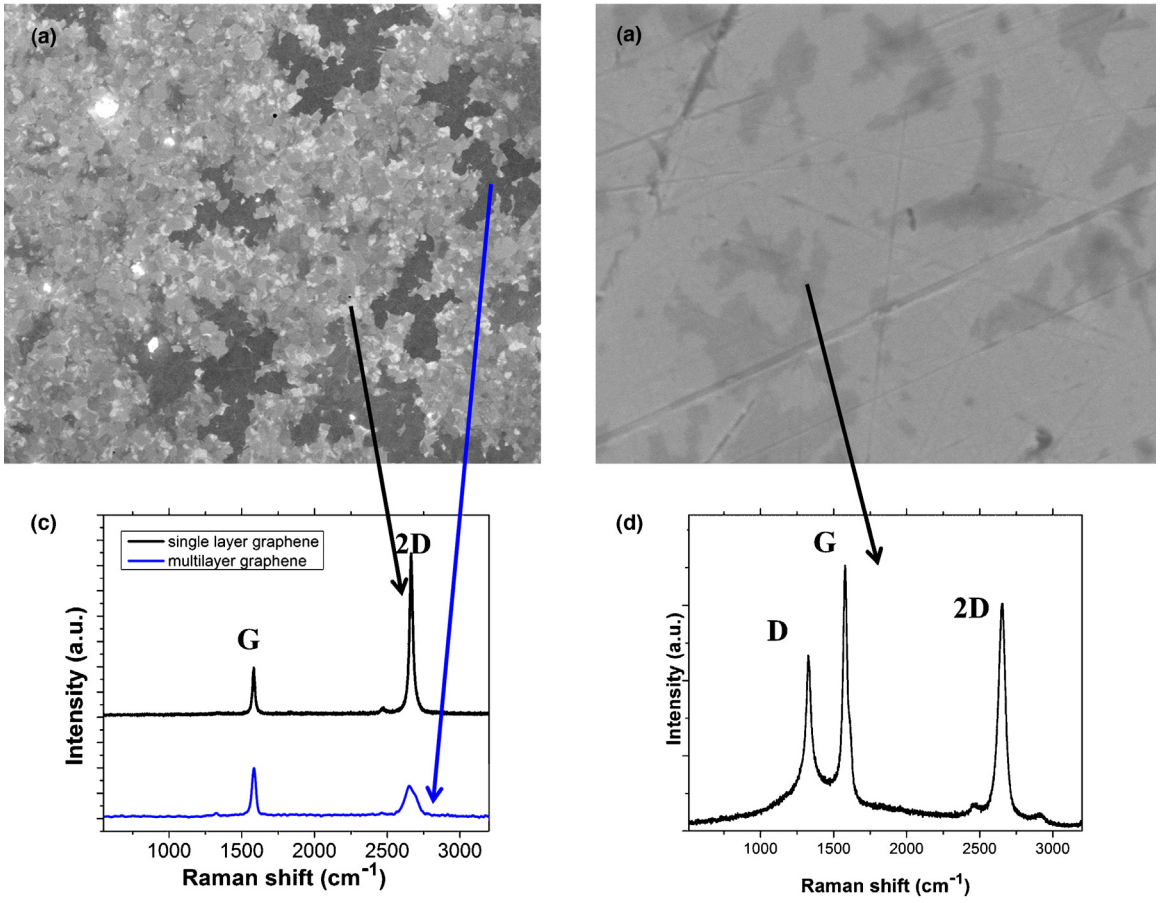


**FIGURE 1**

Scanning electron microscopy images and corresponding Raman spectra for (a and c) CVD-grown multilayer graphene and (b and d) graphene deposited on steel from solution. Raman signatures indicate defect peak presence only for solution-processed graphene (d).

sliding on a surface of graphene layers (which simulates AFM lateral force measurements) and (b) the friction between the graphene layers themselves. In case (a), it was shown that the friction decreases with increase of the number of layers [23,25], while in case (b) the friction was found to behave in the opposite way, achieving higher friction or stick-slip behavior once the number of layers increased to more than three [21,22].

As shown in Fig. 2 [25], the modeling of the AFM tip-graphene interactions, where the lateral force was calculated as the sum of *y*-components of all van der Waals forces acting between the atoms of the CNT tip and those of graphene layers, demonstrated that the friction force decreases as the number of layers increases; that conclusion was also supported by the experimental AFM measurements [27]. That friction is dominated by the contribution from out-of-plane deformation, the so-called mechanism of 'puckering' in front of the scanning tip (Fig. 3d), which increases the contact area and, therefore, the amount of friction. Once the number of graphene layers increases, the interlayer interactions minimize the puckering effect and thereby reduce the friction. Moreover, in Ref. [23], Liu and Zhang stated that not only the increased number of layers, but also the increased tip-surface distance decreases the coefficient of friction for the sliding tip-surface interactions.

The great majority of experimental studies of graphene tribology at the nano-scale have used lateral force AFM or friction force microscopy (FFM) [28–33].

The AFM lateral force measurements demonstrated the friction dependence on the number of graphene layers [27,29,31], in agreement with the predicted behavior in the simulation work reviewed above. Li et al. [5,27] performed FFM studies in ambient conditions using silicon probes. Both free-standing graphene and graphene mechanically transferred on $SiO_2$ showed a decrease in friction with number of layers (Fig. 3) perhaps due to 'puckering' effect. However, if the graphene layer is strongly bonded to the substrate (as was seen in the case of mica substrate [27]), the strong dependence of friction on the number of graphene layers is not observed. Such friction dependence on the number of layers occurs not only in graphene but in all atomically thin lamellar materials. [5,29]

## Micro-scale studies

Even though the transition between the nano-scale and micro-scale is not perfectly evident, we review below the tribological studies of graphene properties performed at small scales by techniques other than AFM.

Kim et al. [34] investigated the adhesion and friction properties of graphene at the micro-scale using a micro-tribometer. Graphene deposited on Ni and Cu substrates by CVD was transferred onto $SiO_2$ substrates, and tribotests were performed in an ambient environment at room temperature using fused silica and polydimethylsiloxane (PDMS) lenses as counterparts. The contact loads

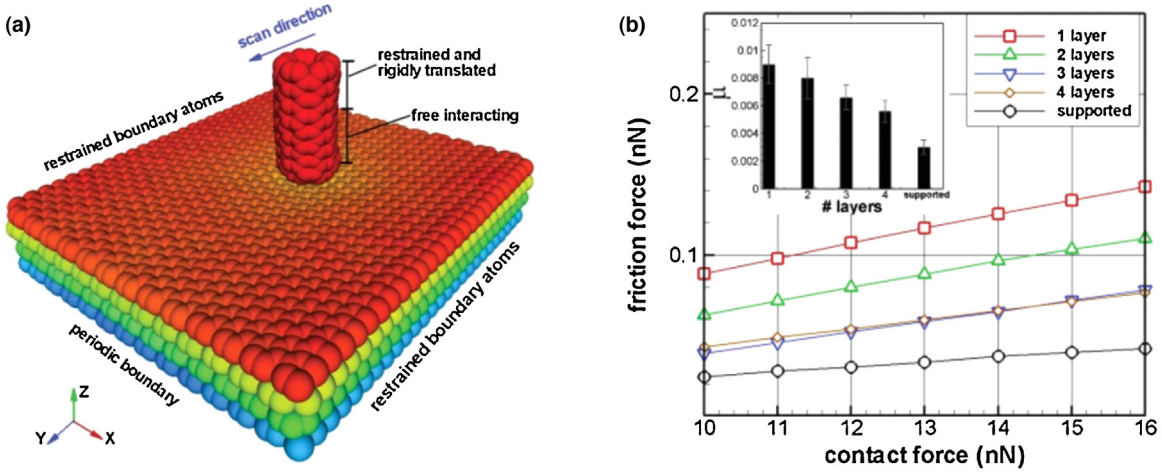


**FIGURE 2**

(a) Four-layer suspended graphene assembly. The color of each atom is determined by its *Z*-position. (b) Contact force vs. friction force and the corresponding friction coefficients as function of number of layers. The results are obtained from Brownian dynamics simulations that model AFM lateral force measurements between the single-wall capped carbon nanotube tip (height and diameter were 2.3 and 1.2 nm, respectively) and suspended few-layer graphene (5.5 nm × 6.2 nm). The contact force was kept at the level of 10–16 nN. The simulations were thermostated at 300 K. Inset shows coefficient of friction versus number of layers. Reprinted figure with permission. Copyright (2012) by the American Physical Society [25].

ranged from 5 to 70 mN. The results demonstrated that both adhesion and friction force are reduced once the $SiO_2$ surface is covered with graphene (Fig. 4). The variation in the properties of graphene grown on different metals is attributed to the weaker adhesion between Cu-grown graphene and the $SiO_2$ surface, resulting in easily worn graphene, even at 5 mN loads.

Shin et al. [35] conducted micro-scale scratch tests as another way for measuring the coefficient of friction of exfoliated and epitaxial graphene at the micro-scale. Results showed that at this scale the coefficient of friction stayed at ~0.03 irrespective of the number of layers. On the basis of both micro and nano studies, the authors attribute the difference in friction dependence on the thickness of the graphene films to the environment and the probe size. Moreover, introduction of defects (provided by oxygen plasma) increased the graphene friction. Therefore, differences can also arise from a defective or non-perfect top layer on the graphene film. Conversely, if the oxidation level of graphene oxide is decreased, as it was shown by Ou et al. [36] for chemically reduced graphene oxide nanosheets on the silicon substrate, the adhesive force is also reduced and this resulted in lowering of the friction.

## Modified graphene studies

The change in the tribological performance of graphene as a function of surface chemistry was of obvious interest. Therefore, the tribological properties of chemically modified graphene

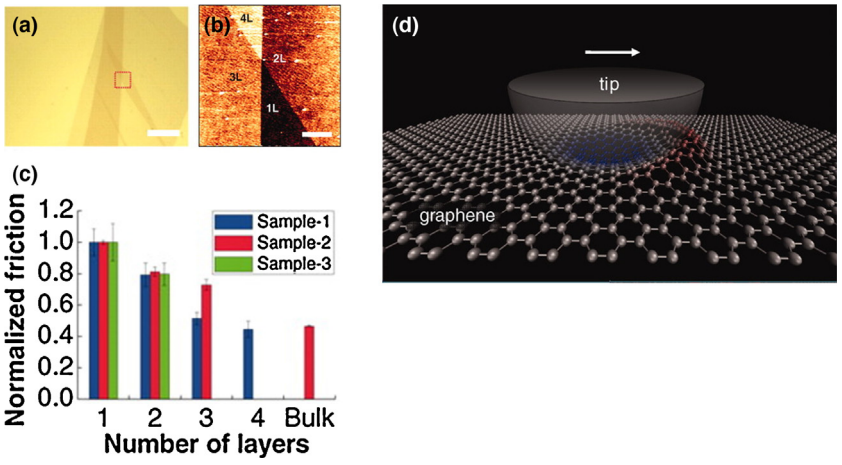


**FIGURE 3**

(a) Bright-field optical microscope image of graphene sample. The red dotted square represents the subsequent AFM scan area. Scale bars, 10 μm. (b) Topographic and friction (forward scan) images measured simultaneously by AFM from the indicated areas. 1 L, 2 L, 3 L, etc. indicate sheets with thicknesses of one, two, three, etc., atomic layers. Scale bars, 1 μm. (c) Friction on areas with different layer thicknesses. For each sample, friction is normalized to the value obtained for the thinnest layer. Error bars represent the standard deviation of the friction signals of each area. In the chart, the same color represents data from the same sample. (d) A schematic showing the proposed puckering effect, where adhesion to the sliding AFM tip creates out-of-plane deformation of a graphene sheet, leading to increased contact area and friction; the color scale of the atoms indicates their out-of-plane positions. Reprinted with permission from AAAS [5].

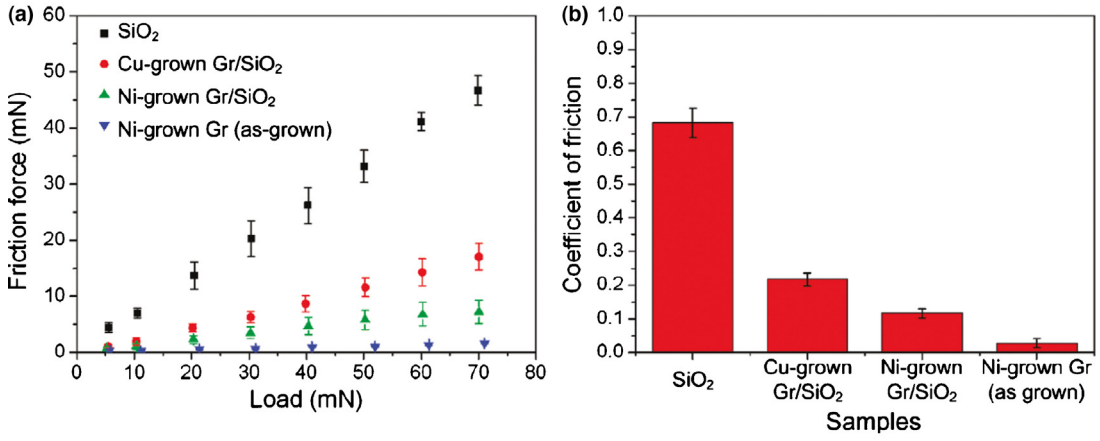


**FIGURE 4**

(a) Friction force as a function of load and (b) coefficient of friction for graphene samples. Only the fused-silica lens was used as a counterpart material in the friction tests. The coefficient of friction was calculated by dividing the friction force by the load. The error bars in both graphs indicate standard deviation. Gr, graphene. Reprinted with permission. Copyright (2011) American Chemical Society [34].

(fluorinated, hydrogenated, or oxidized) were investigated experimentally as well as theoretically by density functional theory (DFT) calculations [37,38].

For oxidized graphene [37] the friction between two sliding graphene layers increases with the introduction of epoxide and hydroxyl groups, and is dominated by electrostatic and non-stable hydrogen bond interactions. The oxide system should overcome a much larger energy barrier due to hydrogen bond formation, thus resulting in high energy dissipation.

By contrast, for the single-side hydrogenated graphene sheets, the friction decreases greatly in comparison with pure graphene [38]. The DFT calculations for normal loads varying from 1 to 9 nN predicted the coefficient of friction to be in the range of 0.01–0.05 when hydrogen bonds are introduced. The lower friction is explained by electrons accumulated between the carbon atom and the attached hydrogen atom, resulting in the repulsion of two interacting sheets and thus in decreased energy of interaction.

For the interactions of two sliding surfaces, because no out-of-plane mechanical stresses are applied, the frictional changes are limited to the ones due to in-plane stresses. In the case of the tip interaction with the graphene surface, the out-of-plane stresses play an important role. Friction force microscopy measurements using a conductive AFM tip [39,40] demonstrated that the nano-scale friction increased in comparison to pristine graphene by two, six, and seven times for hydrogenated, fluorinated, and oxidized graphene, respectively (Fig. 5).

Despite the friction increase for modified graphene, the adhesive properties were shown to decrease for fluorinated graphene or remain almost unchanged for hydrogenated and oxidized graphene with chemical changes due to reduction of the van der Waal's contact area. This finding demonstrates that other factors than adhesion can play an important role in the tribological behavior of the interfaces. Ko et al. [39] suggest that mechanical properties dramatically change with sp3-hybridization arising from chemical modifications of graphene, and this fact plays the major role in the nano-scale friction increase. In addition to in-plane stiffness and adhesion energy reduction, the chemical modification reduces the out-of-plane flexibility of graphene, which is associated with the increase of normal and bending stiffness of the modified graphene. For fluorinated, hydrogenated,

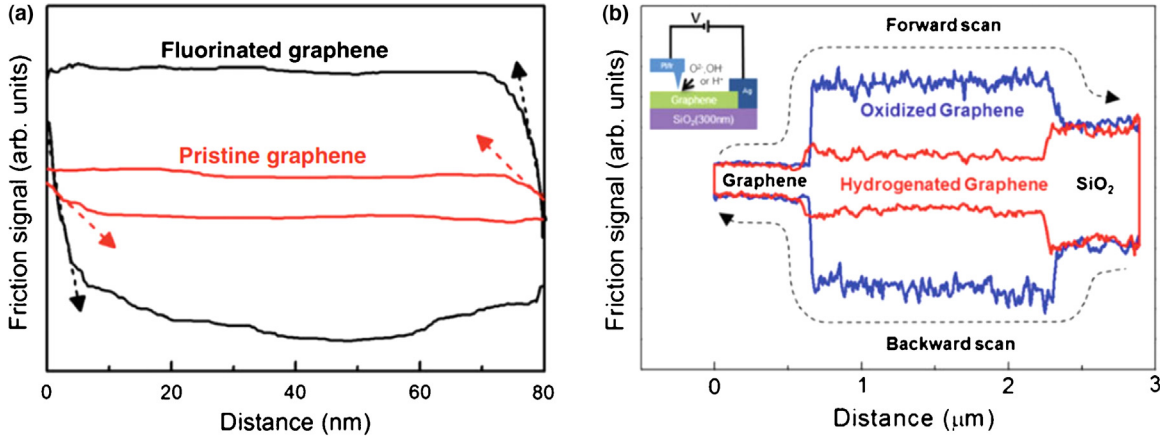


**FIGURE 5**

(a) Friction profiles measured on pristine and fluorinated graphene (applied load of 70 nN). (b) Friction profiles obtained from forward and backward scans across $SiO_2$ and single-layer graphenes, including pristine, oxidized, and hydrogenated areas. The inset shows the experimental scheme of the oxidation and hydrogenation of graphenes. Copyright (2013) from Springer [39].

TABLE 1

**Overview of macroscale tribological properties of widely used solid lubricants.**

| Solid lubricant coating | Deposition methods | Coating thickness (μm) | Typical friction coefficient | Wear/friction mechanism |
|---|---|---|---|---|
| **Graphite** | Evaporation, pyrolysis | 0.2–5 | Dry: 0.5–0.6; Humid: 0.1–0.2 | Interlayer shear and water intercalation |
| **Diamond like carbon (near frictionless carbon)** | Sputtering (rf and dc), ion-beam, PECVD | 1–3 | Dry: 0.001–0.05; Humid: 0.2–0.3 | High chemical inertness and repulsive forces due to hydrogen termination |
| **Tetrahedral amorphous carbon** | Ion beam, cathodic arc, pulsed laser | 0.01–1 | Dry: 0.7; Humid: 0.1 | Tribochemically induced surface reaction and termination of top carbon atoms |
| **Ultrananocrystalline diamond** | MPCVD, HFCVD | 0.5–1.5 | Dry: 0.05–0.13; Humid: 0.007–0.1 | Tribochemically induced reaction with H, O, or OH |
| **$MoS_2$ and $WS_2$** | Sputtering (rf and dc), thermal evaporation CVD, ALD | 0.2–2 | Dry: 0.02–0.06; Humid: 0.15–0.25 initial and increasing | Interlayer shear and transfer film formation |
| **Graphene/graphene oxide** | CVD, chemical and mechanical exfoliation | 0.001–0.002 | Dry: 0.15–0.2; Humid: 0.15–0.2 | Interlayer shear and prevention of tribocorrosion |

and oxidized graphene, the out-of-plane flexibility drives the overall increase in friction.

### *Macro-scale tribology*

Macro-scale friction studies are of direct interest to various industries where material losses due to wear as well as energy wasted due to friction are of great concern. Different bulk solid lubricants and their thin coatings have been used for friction and wear control in the past. Table 1 modified from [3,41] provides quick overview of other known solid lubricant materials widely used by various industries worldwide with the new potential solid lubricant based on graphene.

Surprisingly, less research has been conducted on the tribological properties of graphene at the macro-scale as compared to the nano-scale and micro-scale. We summarize in the following sections the macro-scale lubrication properties of carbon materials, such as graphene, graphene oxide, and graphite, when they are not intentionaly bonded to the surface of interest.

## Graphite vs. graphene: how different is graphene?

Most tribological studies on graphene have been carried out at the nano-scale and micro-scale, building the case for graphene to be used as a solid lubricant. Recent meso-scale and macro-scale tribological investigations confirm previous predictions and open up new opportunities for graphene use as a solid lubricant in macro-scale systems too. Here, we look at graphite in order to better understand how graphene behaves differently tribologically at the macro-scale compared with bulk graphite.

Graphite as a macro-scale solid lubricant has been widely studied and has been used in industry for more than 40 years [42,43]. It is well known that bulk graphite (a source of graphene) works the best in humid environments but fails to provide low friction and wear in inert, dry, or vacuum environments [44]. The reason for this behavior is the intercalation of water molecules between the graphite sheets, which allows easy shearing of graphite and provides low friction. Additionally, previous tribological studies using graphite flakes have indicated formation of graphite scrolls at the tribological interface [45]. These scrolls are favorable for decreasing the surface energy [46,47] and reducing friction in the sliding interfaces.

For the purpose of comparison, in our recent work the graphite powder was mixed in ethanol (5 wt%, which is much larger than the concentration of graphene in ethanol) to reproduce the identical deposition procedure as the one mentioned in 'Graphene as a solid lubricant' section below. The tribological tests were performed in humid air and dry nitrogen under the same test conditions that were used for the graphene studies. As expected, graphite powder did not work well in dry nitrogen, showing high friction and high wear losses (Fig. 6a).

One of the major objectives of this study was to ascertain whether graphene behaves similarly to bulk graphite under dry and inert test conditions. For this graphene study, in addition to a dramatic reduction of friction when graphene is present at the sliding interfaces, the wear is reduced significantly irrespective of the environment. These results (Fig. 6b) demonstrate the unique properties of graphene as a solid lubricant regardless of dry and humid test environments. This quality is unique to graphene and not possible with polycrystalline graphite or HOPG. To demonstrate the stable behavior of the coefficient of friction when graphene is applied on the steel surface, we performed the various tests: that is, changing the relative humidity by filling the test chamber with dry nitrogen to achieve ultra-dry test conditions and opening the test chamber to achieve humid air conditions. In every case, we repeatedly found unique behavior of graphene, showing low friction and wear in humid and dry environments. The macro-scale lubricative properties of graphene are discussed in more detail below.

## Graphene as a solid lubricant

Previous studies [48,49] demonstrated the unusual friction and wear properties of a few graphene layers on the steel surfaces. Specifically, a small amount of solution-processed graphene (SPG) was deposited from low concentration ethanol solution (1 mg/L) with only partial coverage of the steel surface (~25% of the total surface area), which was sufficient to reduce both friction and wear in the dry nitrogen and humid air environments (Fig. 7). In the dry

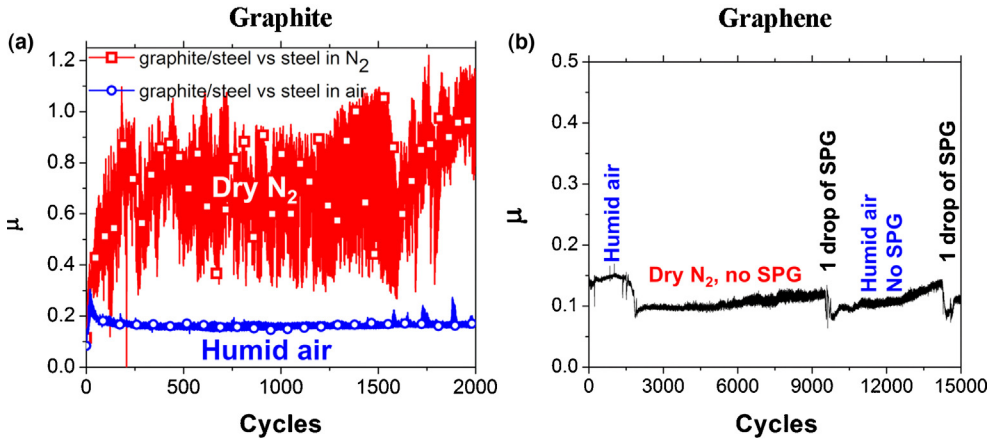


**FIGURE 6**

(a) Coefficient of friction for graphite deposited on steel from ethanol solution for tests performed in humid air and dry nitrogen. (b) Interchangeable behavior of graphene protection in dry and humid environments. The applied load is 1 N.

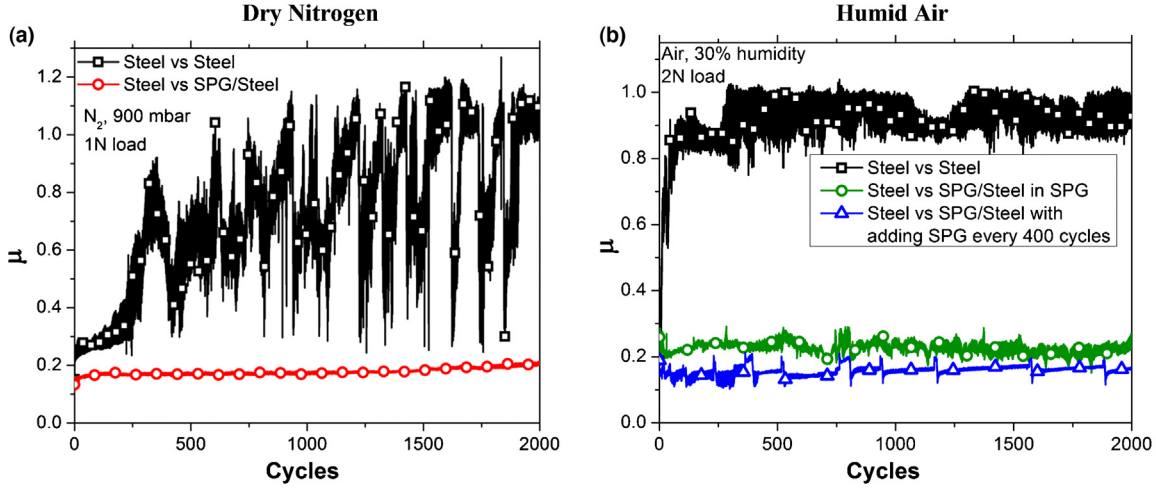


**FIGURE 7**

Coefficient of friction (μ) for (a) SPG/steel and bare steel sliding interfaces in nitrogen and (b) self-mated steel test pair in humid air without SPG or ethanol, in ethanol solution with SPG, and in ethanol solution with intermittent supply of SPG. Reprinted from Carbon 54, Berman et al. Copyright (2013) [48].

nitrogen and humid air, the few layers of graphene demonstrated stable low friction (coefficient of friction equal to 0.15 in comparison to ~1 for bare steel) and four orders of magnitude reduction in wear in comparison to bare steel. Even in dry nitrogen, the coefficient of friction of the graphene layer derived from ethanol solution is comparable to that of HOPG in humid environments [42,44]. Tests performed in the humid air required replenishing the graphene layer in the wear track for stable low friction and low wear regime. The results clearly demonstrated the wear protection qualities of graphene layers, especially when SPG is periodically fed to the sliding interfaces.

The tribotests as a function of increasing load showed that the lifetime of the graphene protective layer is shorter under higher loads, as illustrated in Fig. 8a. As is clear, the lifetime in dry nitrogen decreases to a few hundred cycles for 5 N load (or 0.56 GPa), while under low load condition (i.e., 1 N) the graphene protection is more durable. The graphene protective layer at 1 N load (Hertz contact pressure of 0.33 GPa) was shown to last without replenishment as long as 6000 cycles before the flakes of graphene started to be pushed outside of the wear track, with complete removal of the graphene layer at around 14,000 cycles.

To understand the mechanism behind the friction and wear reduction of the graphene lubricant, the wear tracks of the initial sliding low-friction regime and the follow-up high-friction stage were analyzed with Raman spectroscopy using a 633 nm red laser. The results demonstrated that at the initial stage, where the coefficient of friction is low and stable, graphene forms a uniform coating within the wear track area (Fig. 8b). The presence of a graphene layer everywhere at the wear track is confirmed with Raman mapping of the 2D peak (~2700 $cm^{-1}$, red color corresponds to the highest intensity, blue to the lowest when no peak is present).

The Raman analysis of the wear track for the regime when the coefficient of friction is high and non-stable reveals that the majority of the graphene layers are worn out or removed from the wear track, thus indicating the presence of graphitic flakes near the track (Fig. 8c). In this case the 2D peak (at ~2700 $cm^{-1}$) of graphene is weak while the defect peak D (at ~1350 $cm^{-1}$) is much

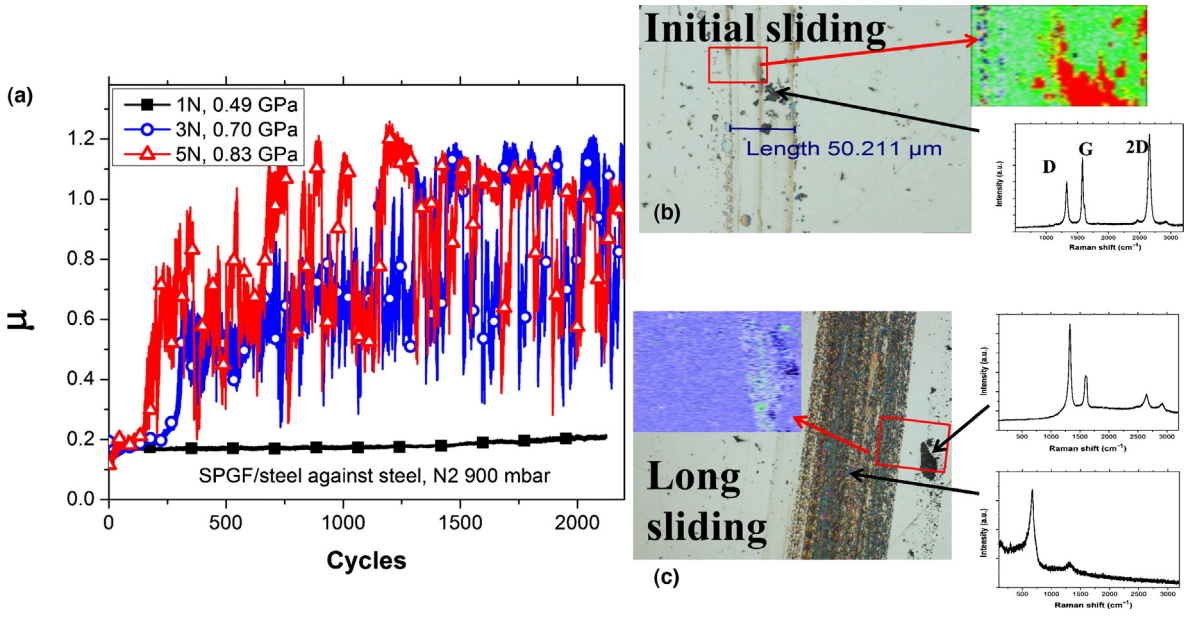


**FIGURE 8**

(a) Coefficient of friction for steel with SPG under different loads for 2000 cycles in dry nitrogen. Raman signatures for (b) initial cycling with graphene protecting the wear track and (c) long cycling with graphene removed from the wear track. Reprinted from Carbon 59, Berman et al. Copyright (2013) [49].

stronger, suggesting that graphene is converted to a disordered graphitic structure due to modifications during sliding. The presence of iron oxides (at ~1300 $cm^{-1}$ and 1600 $cm^{-1}$) and nitrides (at ~673 $cm^{-1}$ and below) in the wear track itself is confirmed by Raman analysis, indicating severe damage and corrosion of the steel when the graphene layer is removed from the wear track.

It is important to mention that for both dry nitrogen and humid air, as long as graphene is present at the sliding steel interfaces, the friction is reduced by 5–6 times and wear by four orders of magnitude for more than 15,000 wear cycles. Graphene as a two-dimensional material not only shears easily at the sliding contact interfaces but also provides protection against corrosion and oxidation, which can, in turn, help reduce friction and wear.

## Graphene oxide vs. graphene

To complete the picture of the macro-scale properties of graphene, we also reviewed the role of chemically modified graphene, namely, graphene oxide. In a model experiment, solution-processed graphene oxide (SPGO) sheets in a highly concentrated water solution (5 g/L) were deposited onto highly polished steel surfaces. For the dry nitrogen environment tests, the water was evaporated to leave graphene oxide flakes on the steel surface. In the case of tests performed in a humid air environment, the sliding tests were performed in a water solution to ensure a sufficient supply of graphene oxide during the whole test procedure. Fig. 9 shows X-ray photon spectroscopy and Raman spectra for the SPGO and SPG layers. Both for graphene and graphene oxide the survey scan (shown in the inset) indicates the presence of oxygen on the surface of the protected steel surface (28 at% for graphene flakes and 43 at% for graphene oxide layers). However, the higher-resolution C1s spectra confirm that most of oxygen is chemically bonded to the carbon in the case of SPGO (C–O and C═O peaks), and very small amount of oxygen is bonded to carbon for SPG (only small C═O peak is detected, possibly due to the oxygen bonded at the defect sites), consistent with previous XPS studies on graphene and graphene oxide mentioned in the literature [50]. Raman spectrum in Fig. 9c and d shows typical Raman signature of graphene (SPG) and graphene oxide (SPGO) respectively.

The tribological behavior of graphene oxide layers at macroscale is found to be not much different from that of the graphene layers, which is in contrast to the nano-scale and micro-scale studies on graphite oxide indicating different mechanism at play and needs further investigations to understand the exact mechanism. Fig. 10 shows the coefficient of friction and optical image of the wear track for the tests carried out using SPGO in dry and humid environments. The results confirm that graphene oxide may also be used to lubricate steel at macroscale by providing the COF below 0.2. However, the wear rate stays at higher level than the ones for unmodified graphene. The further wear rate comparison is presented in the following 'Comparison of wear for graphite, graphene, and graphene oxide' section.

## Comparison of wear for graphite, graphene, and graphene oxide

Fig. 11 summarizes the coefficient of friction and wear for uncoated steel and steel coated with graphite, graphene, and graphene oxide (1 N load, 2000 sliding cycles). For all three coatings, the amount of solution was 2–3 drops or 0.1–0.15 mL of solution per 1 $cm^2$ steel; however, the concentration varied from 1 mg/L for graphene, to 10 g/L for graphene oxide, to 50 g/L for graphite.

Even though the coefficient of friction for graphene and graphene oxide in dry nitrogen and humid environments, as well as for graphite in humid air environment, stays at approximately the same level of 0.15–0.17 (Fig. 11), graphene layers provide the best wear protection, suppressing the wear by 3–4 orders of magnitude in comparison to bare steel sliding interfaces. This finding is especially impressive considering that, of the three coatings, the

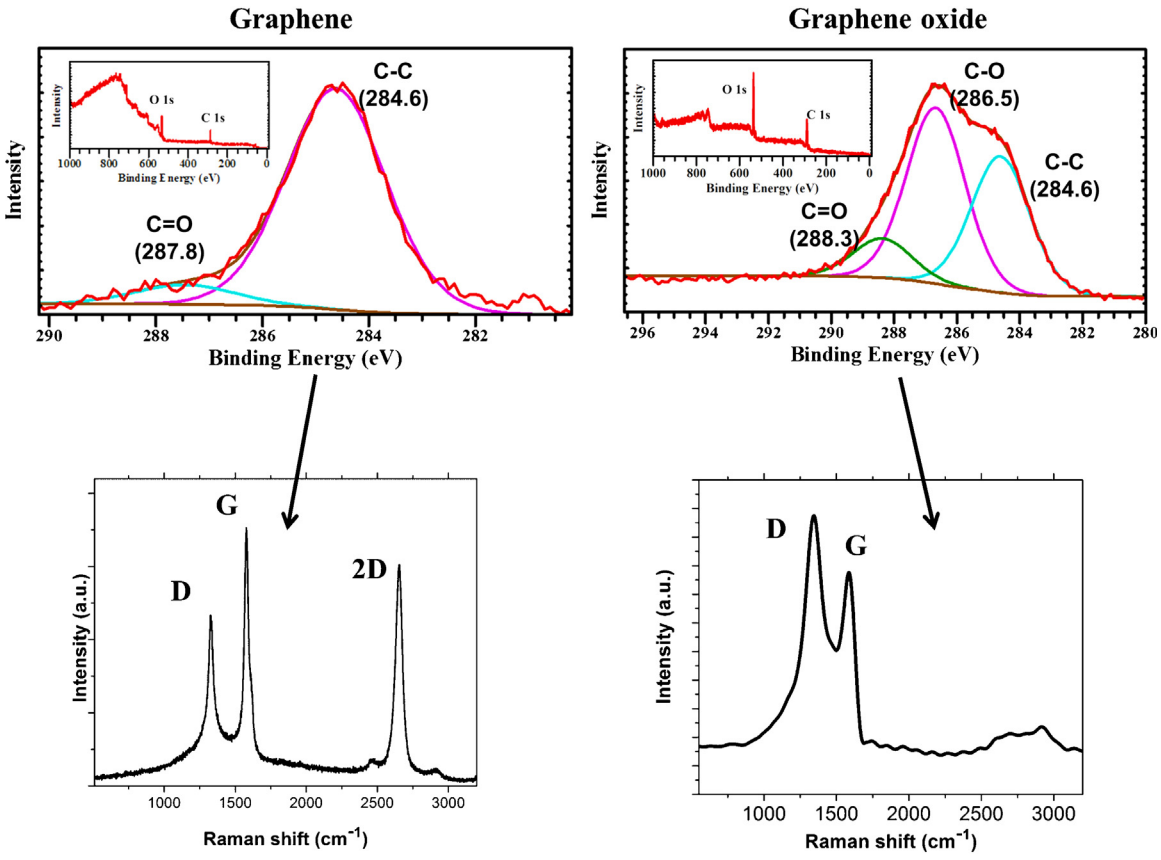


**FIGURE 9**

X-ray photon spectroscopy (a and c) and corresponding Raman signatures (b and d) for solution processed graphene and graphene oxide.

amount of graphene layers from ethanol solution used was the smallest to achieve good, stable lubrication lasting thousands of cycles.

For graphene oxide the wear rate is 1–2 orders of magnitude larger than that for graphene layers. This difference is believed to arise because oxidized graphene does not have as good two-dimensional coverage as graphene, and the oxygen presence in graphene oxide may cause corrosion of steel, thus increasing the wear, while sliding between graphene oxide layers ensures low coefficient of friction. Therefore, the comparably low coefficient of

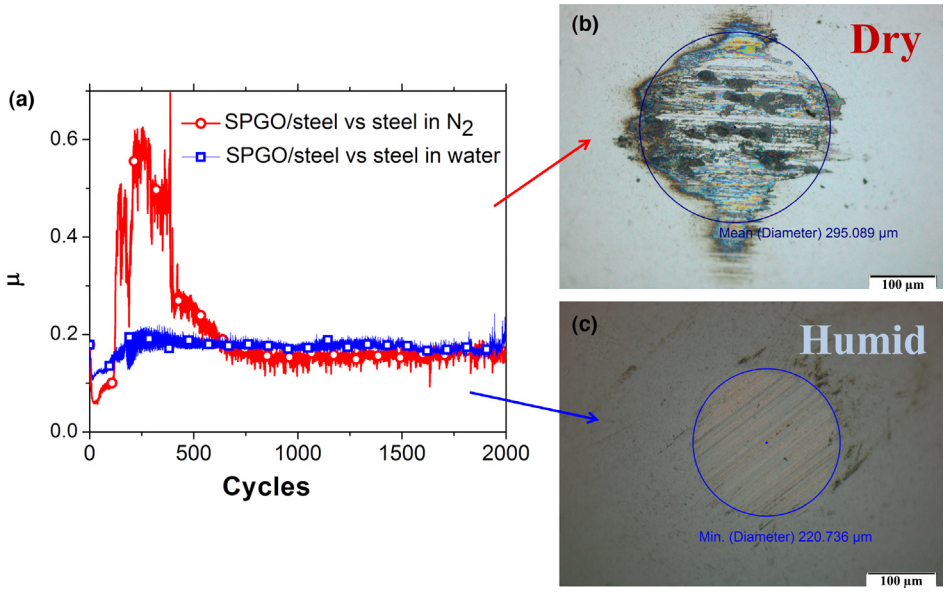


**FIGURE 10**

(a) Coefficient of friction and optical images of the wear track on the steel ball for the tests with SPGO showing (b) wear of in dry and in (c) humid (water solution) environment. The normal load was kept at 1 N, and the sliding speed was 60 rpm (or 9.4 cm/s) at the wear track of 15 mm radius.

| Tribo pair | Test conditions | Calculated Wear Volume | Wear rate (Wear/(load·distance)) | Coefficient of Friction |
|---|---|---|---|---|
| Steel/Steel | Air | $6.8\times10^{-3}$ mm$^3$ | $1.80\times10^{-5}$ mm$^3$/N·m | 1 |
| | Nitrogen | $4.9\times10^{-4}$ mm$^3$ | $1.31\times10^{-6}$ mm$^3$/N·m | 0.9 |
| With SPG | Adding drops/Air | $11.4\times10^{-7}$ mm$^3$ | $3.01\times10^{-9}$ mm$^3$/N·m | 0.15 |
| | Nitrogen | $9.6\times10^{-7}$ mm$^3$ | $2.54\times10^{-9}$ mm$^3$/N·m | 0.15 |
| With Graphite | Air | $1.9\times10^{-5}$ mm$^3$ | $4.94\times10^{-8}$ mm$^3$/N·m | 0.17 |
| | Nitrogen | $1.9\times10^{-4}$ mm$^3$ | $5.07\times10^{-7}$ mm$^3$/N·m | 0.8 |
| With SPGO | Water/air | $2.5\times10^{-5}$ mm$^3$ | $6.51\times10^{-8}$ mm$^3$/N·m | 0.17 |
| | Nitrogen | $7.8\times10^{-5}$ mm$^3$ | $2.08\times10^{-7}$ mm$^3$/N·m | 0.16 |

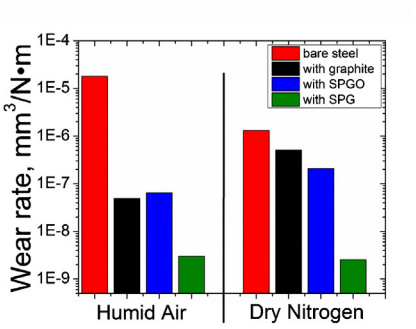


**FIGURE 11**

Wear rate for bare steel, graphite/steel, graphene oxide/steel, and graphene on steel in humid and dry environments. From Refs. [48,49].

friction for graphene oxide does not provide as good wear protection.

For the graphite powder, the low coefficient of friction in humid air can be attributed to the sliding occurring between graphite particles. However, graphite does not produce as good thin film coverage as graphene and does not protect the graphene surface from corrosion, which results in higher wear than that for sliding with graphene layers. Moreover, for graphite to establish a similarly low coefficient of friction requires a much larger amount of material.

### *Graphene as an additive in oils and composite materials*

In addition to being used as a solid lubricant by itself, graphene can be used as an additive in conventional lubricants, such as oils, solvents, and other types of fluids. Results have indicated that even a minimal amount of graphene platelets added to oil [51,52] is capable of noticeable reduction in friction and wear of steel. For chemically modified graphene platelets [51] that were dispersed in base oil by sonication and stirring with a magnet, tribological tests were performed on a four-ball machine with a 1200 rpm speed under constant load of 147 N at the elevated temperature of 75 °C. The optimal 0.075 wt% weight amount of modified graphene platelets was able to provide a better load-carrying capacity than a base oil or oil with graphite flake additive. Both the coefficient of friction and wear reduced with the added graphene platelets (Fig. 12).

Adding 0.1 wt% graphene oxide nanosheets to oil was also [53] able to reduce friction and wear at high loads and different temperatures. For instance, the average coefficient of friction decreased by 20% in comparison to that of pure oil at the contact pressure of 1.17 GPa and temperature in the range 25–80 °C. The wear scar diameter was also reduced from 10% to up to 30% when graphene oxide nanosheets were introduced.

Graphene platelets are able to reduce the wear of other solid lubricants. Kandanur et al. [54] demonstrated that the wear rate of polytetrafluoroethylene (PTFE) was reduced by four orders of magnitude when 10 wt% of graphene platelets was incorporated as nano-fillers. In this study graphene platelets, consisting of 3–4 graphene sheets, were obtained by thermal exfoliation and reduction of graphite oxide. The authors showed that the wear rate reduces as platelets are introduced to 'Teflon'. Kandanur et al. [54] suggested that, initially, PFTE suffers high wear due to distribution of sub-surface cracks propagating parallel to the sliding interface and connecting eventually with the surface, while fillers are able to interfere with the formation of cracks, thus deflecting them and limiting the wear.

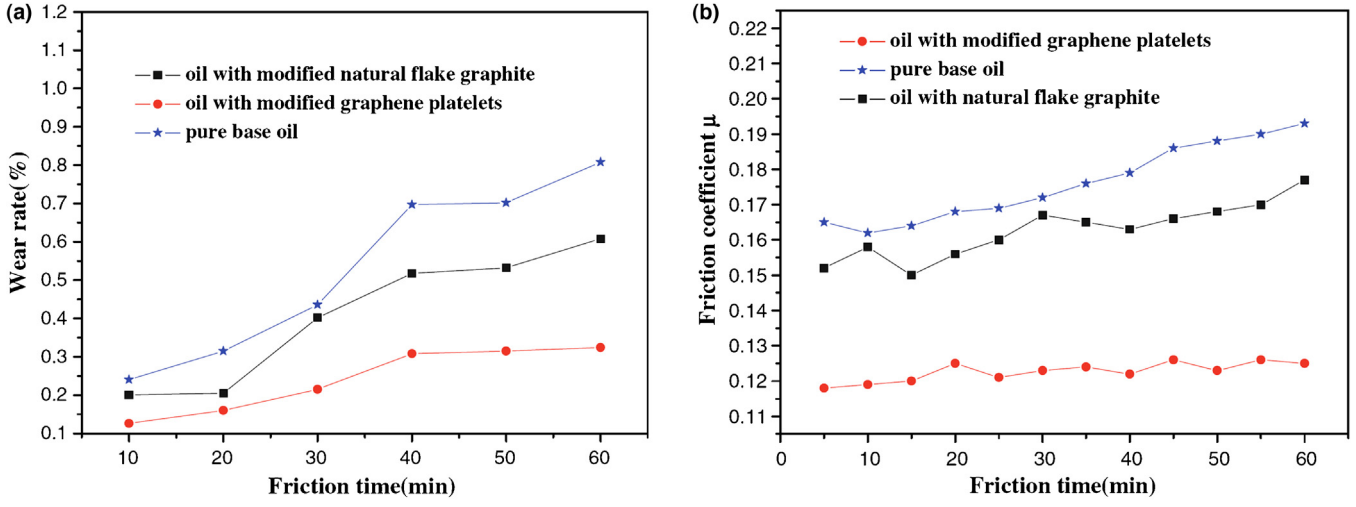


**FIGURE 12**

(a) Wear rate as a function of friction time (four-ball, 1200 rpm, 147 N, 60 min, 75 ± 2 °C). (b) Friction coefficient as a function of friction time (four-ball, 1200 rpm, 147 N, 60 min, 75 ± 2 °C). Copyright (2011) from Springer [51].

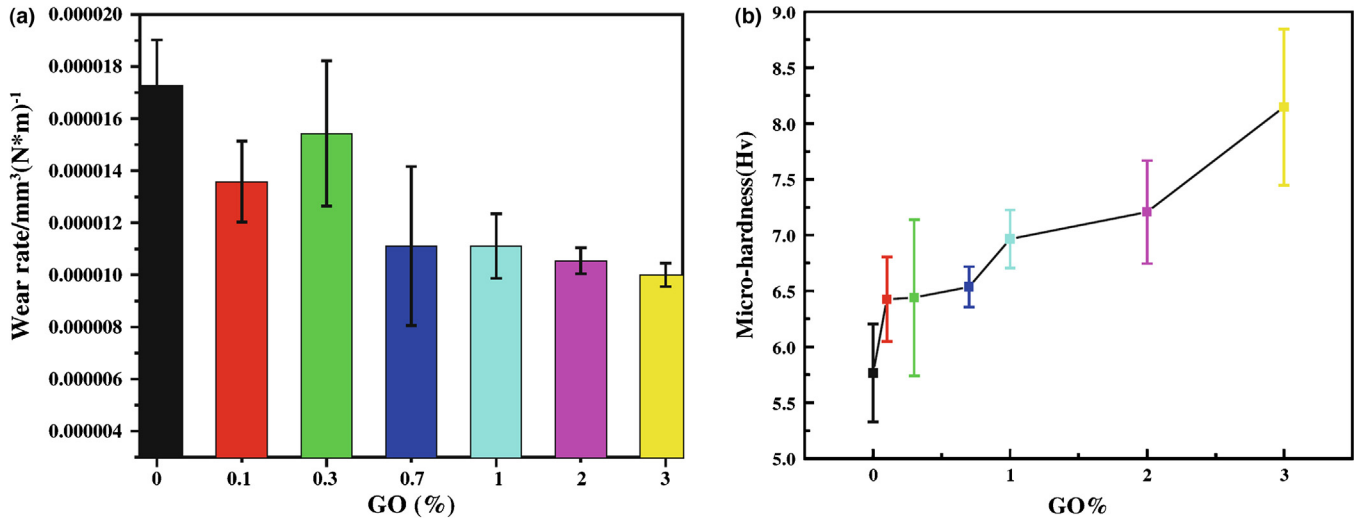


**FIGURE 13**

(a) Variation of wear rate of the GO/UHMWPE composites as a function of GO content after the wear tests. (b) The microhardness of GO/UHMWPE composites with the different GO contents. Copyright (2011) from Springer [55].

Dramatic reductions are attained on the wear rates of of ultra-high molecular weight polyethylene (UHMWPE) composites by adding graphene oxide nanosheets at a range of concentration from 0.1 to 3 wt% as shown in Fig. 13. UHMWPE is used widely as a bearing material for hip and knee implants [55]. Even though the friction coefficient slightly increases, the wear is reduced by 40% when the content of graphene oxide in UHMWPE reaches 3 wt% (Fig. 13). This wear protective effect is attributed to increased tendency to form a protective transfer film and increased mechanical strength and hardness, which limit microcrack initiation and growth and thus wear of UHMWPE during sliding.

Organic solvent lubricants may also benefit from adding graphene. Choudhary et al. [56] prepared alkylated graphene with variable alkyl chain length by coupling of alkylamine with carboxylic groups of graphene oxide and then dispersed it in different organic solvents. They showed that during alkylation the size of the sp2 carbon domains increases, thus confirming reduction in oxidized graphene. The tribological tests using a four-ball machine confirmed friction and wear reduction of steel in hexadecane when 0.06 mg/mL of graphene nanosheets is introduced. In the tests performed under 392 N load at the speed of 1200 rpm at temperature 75 °C, the friction and wear were reduced by 26% and 9%, respectively. The enhancement in lubrication properties is attributed to the supply of graphene nanosheets between the rubbing surfaces, which prevent the direct contact of steel and provide low resistance to shearing.

## Conclusions

This review highlights the recent developments regarding the use of graphene as a lubricant for nano-scale to macro-scales. In particular, research showing graphene's superior tribological properties compared with graphite and graphene oxide is covered. Further, recent studies dealing with graphene as an additive for lubricating oils and for the fabrication of self-lubricating nanocomposite materials are presented. These dedicated studies have confirmed the following key findings.

- Theoretical simulations predicted that the low friction of graphene is highly dependent on the sliding interfaces (whether the tip is sliding on the graphene surface or two graphene surfaces are sliding against each other) and on the number of graphene layers.
- AFM studies confirmed the theoretical prediction of decreasing friction when the number of layers is increased. Moreover it was shown that friction can reach the ultra-low friction regime at specific loads when the sliding occurs without stick-slip.
- Micro-scale tribological studies showed that introduction of defects in graphene increases friction. Also, chemical modifications of graphene by hydrogenation, fluorination, or oxidation result in 2, 6, and 7 times increase in friction, respectively.
- Macro-scale tribological studies clearly demonstrated how graphene is different from graphite in reducing friction and wear irrespective of atmospheric conditions (humid or dry) and also acting as a perfect passivation layer inhibiting the corrosion induced wear (tribo-corrosion) in case of steel contacts.
- Macro-scale studies demonstrated that graphene layers largely suppress the friction and wear of the sliding steel interfaces. Thus, the friction of steel drops from 0.9 to 1 for bare steel down to 0.15–0.16 for graphene coated steel in dry nitrogen and humid air environments. The wear volumes and rates are reduced by 3–4 orders of magnitude when graphene is present at the sliding interfaces.
- Overall in this review, graphene was shown to be very effective for friction and wear reduction not only as a lubricant but also as an additive to oils, composite materials and solvents.

## Acknowledgments

Use of the Center for Nanoscale Materials was supported by the U. S. Department of Energy, Office of Science, Office of Basic Energy Sciences, under Contract No. DE-AC02-06CH11357.

## Appendix A. Instrument citation

Macro-scale tribological tests were performed in humid air (30% RH) and dry nitrogen (900 mbar) at room temperature using a CSM tribometer with a ball-on-disk contact geometry. Stainless steel flat samples (440C grade) with rms roughness $R_q = 20$ nm

were initially cleaned by sonication in acetone and then in isopropanol alcohol. The counterpart was a stainless steel ball (440C grade) of 9.5 mm diameter with rms roughness measured by the 3D profilometer $R_q$ = 15 nm. The normal load during the tribotests was varied from 1 N up to 5 N at a speed of 60 rpm (or 9 cm/s), and the radius of the wear track was 15 mm. The sliding test durations were 2000 cycles or 190 m.

Solution-processed graphene was prepared by chemical exfoliation of highly oriented pyrolytic graphite (HOPG) and was then suspended in ethanol, while solution-processed graphene oxide was suspended in water (Graphene Supermarket Inc.). Raman spectroscopy was performed with an Invia confocal Raman microscope using red laser light ($\lambda$ = 633 nm). The imaging of the wear scars was performed with an Olympus UC30 microscope. The wear rates on the ball and the flat sides were determined with a 3D non-contact MicroXam profilometer.

## References


[1] K. Holmberg, P. Andersson, A. Erdemir, Tribol. Int. 47 (2012) 221–234.
[2] A. Erdemir, J.M. Martin, Superlubricity, Elsevier, Amsterdam, 2007.
[3] A. Erdemir, in: B. Bhushan (Ed.), Handbook of Modern Tribology, CRC Press, 2001, pp. 787–818.
[4] K.S. Novoselov, et al. Science 306 (2004) 666.
[5] C. Lee, et al. Science 328 (2010) 76.
[6] G.H. Lee, et al. Science 30 (2013) 1073–1076.
[7] J.S. Bunch, et al. Nano Lett. 8 (2008) 2458.
[8] E. Singh, et al. ACS Nano 7 (2013) 3512.
[9] K.S. Novoselov, et al. Proc. Natl. Acad. Sci. U.S.A. 102 (2005) 10451.
[10] D. Chen, L. Tang, J. Li, Chem. Soc. Rev. 39 (2010) 3157.
[11] C. Soldano, A. Mahmood, E. Dujardin, Carbon 48 (2010) 2127.
[12] M. Lotya, et al. ACS Nano 4 (2010) 3155.
[13] S. Mohammadi, et al. Carbon 52 (2013) 451–463.
[14] K.S. Kim, et al. Nature 457 (2009) 706.
[15] X. Li, et al. Nano Lett. 9 (2009) 4268.
[16] P.W. Sutter, J.I. Flege, E.A. Sutter, Nat. Mater. 7 (2008) 406–411.
[17] S.W. Lee, et al. J. Phys. Chem. Lett. 3 (2012) 772–777.
[18] M.H. Rummeli, et al. Adv. Mater. 23 (2011) 4471.
[19] Y.-H. Lee, J.-H. Lee, Appl. Phys. Lett. 96 (2010) 083101.
[20] A.C. Ferrari, et al. Phys. Rev. Lett. 97 (2006) 187401.
[21] L. Xu, et al. Nanotechnology 22 (2011) 285708.
[22] L. Xu, et al. Carbon 50 (2011) 1025–1032.
[23] P. Liu, Y.W. Zhang, Carbon 49 (2011) 3687–3697.
[24] F. Bonelli, et al. Eur. Phys. J. B 70 (2009) 449–459.
[25] A. Smolyanitsky, et al. Phys. Rev. B 85 (2012) 035412.
[26] Y. Guo, et al. Phys. Rev. B 76 (2007) 155429.
[27] Q. Li, et al. Physica Status Solidi B 247 (2010) 2909–2914.
[28] X. Feng, et al. ACS Nano 7 (2013) 1718–1724.
[29] H. Lee, et al. Nanotechnology 20 (2009) 325701.
[30] T. Filleter, et al. Phys. Rev. Lett. 102 (2009) 086102.
[31] L.Y. Lin, et al. Surf. Coat. Technol. 205 (2011) 4868–4869.
[32] Z. Deng, et al. Nature 11 (2012) 1032–1037.
[33] T. Filleter, R. Bennewitz, Phys. Rev. B 81 (2010) 155412.
[34] K.S. Kim, et al. ACS Nano 5 (2011) 5107–5114.
[35] Y.J. Shin, et al. Carbon 49 (2011) 4059–4073.
[36] J. Ou, et al. Langmuir 26 (2010) 15830–15836.
[37] L.-F. Wang, et al. Phys. Rev. B 86 (2012) 125436.
[38] J. Wang, et al. Tribol. Lett. 48 (2012) 255–261.
[39] J.-H. Ko, et al. Tribol. Lett. 50 (2013) 137–144.
[40] S. Kwon, et al. Nano Lett. 12 (2012) 6043–6048.
[41] T.W. Scharf, S.V. Prasad, J. Mater. Sci. 48 (2013) 511–531.
[42] D.H. Buckley, W.A. Brainar, Carbon 13 (1975) 501–508.
[43] J.-A. Ruan, J. Appl. Phys. 76 (1994) 8117–8120.
[44] P.J. Bryant, P.L. Gutshall, L.H. Taylor, Wear 7 (1964) 118–126.
[45] J. Spreadborough, Wear 5 (1962) 18–30.
[46] H. Shioyama, T. Akira, Carbon 41 (2003) 179–181.
[47] J.L. Li, Q.S. Peng, G.Z. Bai, W. Jiang, Carbon 43 (2005) 2817–2833.
[48] D. Berman, A. Erdemir, A.V. Sumant, Carbon 54 (2013) 454–459.
[49] D. Berman, A. Erdemir, A.V. Sumant, Carbon 59 (2013) 167–175.
[50] Y. Jin, et al. Appl. Surf. Sci. 264 (2013) 787–793.
[51] J. Lin, L. Wang, G. Chen, Tribol. Lett. 41 (2011) 209–215.
[52] B.Z. Jang, A. Zhamu, Patent US 8,222,190 B2.
[53] A. Senatore, et al. ISRN Tribol. (2013), 425809.
[54] S.S. Kandanur, et al. Carbon 50 (2012) 3178–3183.
[55] Z. Tai, et al. Tribol. Lett. 46 (2012) 55–63.
[56] S. Choudhary, H.P. Mungse, O.P. Khatri, J. Mater. Chem. 22 (2012) 21032.